

1 **DATA DRIVEN SOLUTIONS AND DISCOVERIES IN MECHANICS**
2 **USING PHYSICS INFORMED NEURAL NETWORK ***

3 QI ZHANG[†], YILIN CHEN [†], AND ZIYI YANG[‡]

4 **Abstract.** Deep learning has achieved remarkable success in diverse computer science appli-
5 cations, however, its use in other traditional engineering fields has emerged only recently. In this
6 project, we solved several mechanics problems governed by differential equations, using physics in-
7 formed neural networks (PINN). The PINN embeds the differential equations into the loss of the
8 neural network using automatic differentiation. We present our developments in the context of solv-
9 ing two main classes problems: data driven solutions and data driven discoveries, and we compare
10 the results with either analytical solutions or numerical solutions using finite element method. The
11 remarkable achievements of PINN model shown in this report suggest the bright prospect of the
12 physics-informed surrogate models that are fully differentiable with respect to all input coordinates
13 and free parameters. More broadly, this study shows that PINN provides an attractive alternative
14 to solve traditional engineering problems.

15 **Key words.** Conservation laws, Data inference, Data discovery, Dimensionless form, PINN

16 **1. Introduction.** It is well-known that many mechanics phenomenons are gov-
17 erned by conservation laws which can be converted to differential equations for most
18 of the applications. Solving these differential equations and obtaining parameter
19 estimations from given observations are always intriguing topics, and significant re-
20 search has been done to develop many advanced (semi-)analytical or numerical algo-
21 rithms. While in the last decade, machine learning especially neural networks have
22 yielded revolutionary results across diverse disciplines, including image and pattern
23 recognition, natural language processing, genomics, and material constitutive model-
24 ing [15, 23, 26, 34], among which a fair amount of research has also been done related
25 to differential equations [1, 9, 12, 13, 17–19, 22, 24, 25, 27–33, 35, 36, 38], owing to the dra-
26 matic increase in the computing resources. Therefore, it will be interesting to adopt
27 neural networks as an important alternative to traditional mathematical methods to
28 approximate the solutions to differential equations through iterative update of the
29 network weights and biases.

30 **2. Related work.** Early researches that use neural network in scientific com-
31 puting could date back to [12, 22], in which a single hidden layer neural network is
32 adopted

33 (2.1)
$$N = \tilde{u} + \sum_{i=1}^H v_i \sigma_i \left(\sum_{j=1}^n w_{ij} x_j + u_i \right),$$

34 where N is the network output which is assumed to be a scalar for illustration pur-
35 poses, H is the width of the hidden layer, and n is the dimension of the input vector
36 $\mathbf{x} \in \mathbf{R}^n$, w_{ij} and v_i are called weights while u_i and \tilde{u} are always denoted as the bi-
37 ases, $\sigma_i(\cdot)$ is called activation function. More recently, the development of automatic
38 differentiation [2] has led to emerging literature on the use of deep neural networks
39 to solve differential equations [17, 33, 38, 39] even in complex geometries, and Berg

*Stanford CS229 project final report, category of physical sciences

[†]Department of Civil and Environmental Engineering, Stanford University, CA 94305
(qzhang94@stanford.edu, yilinc2@stanford.edu).

[‡]Department of Mechanical Engineering, Stanford University, CA 94305 (zy99@stanford.edu).

40 et al. [3] provides details of this back propagation algorithm for advection and diffu-
 41 sion equations. Unlike traditional machine learning methods, deep neural networks
 42 sometimes can overcome the curse of dimensionality [17]. In the work done by Raissi
 43 et al [30–32], they named such strong form approach for differential equation as the
 44 physics-informed neural network (PINN) for the first time. Today, the PINN becomes
 45 more and more popular in many engineering fields such as hydrogeology [7, 18, 35],
 46 geomechanics [19], cardiovascular system [21] and so on. One attractive feature of
 47 PINN is that it is fully differentiable with respect to all the input coordinates and
 48 free parameters, in other words, the trial solution (via the trained PINN) represents
 49 a smooth approximation that can be evaluated and differentiated continuously on the
 50 domain [9]. Another important feature of PINN is that it can be used to solve inverse
 51 (data discovery) problems [16] with minimum change of the code from the forward
 52 problems [24].

53 It is also worth to mention that there are also other machine learning methods
 54 that didn't rely on the neural network to solve differential equations [28, 29], but in
 55 this report, we will focus on the PINN.

56 **3. Methods.** In this section, we will give a very brief overview of PINN in order
 57 to demonstrate how the loss function \mathcal{L} is defined in such context. We refer interested
 58 readers to look at [32] for more details. Consider a system of differential equations
 59 defined on the domain Ω with boundary $\partial\Omega$:

$$60 \quad (3.1) \quad \mathcal{D}(\mathbf{u}(\mathbf{x})) = \mathbf{0} \quad \mathbf{x} \in \Omega,$$

61

$$62 \quad (3.2) \quad \mathcal{B}(\mathbf{u}(\mathbf{x})) = \mathbf{0} \quad \mathbf{x} \in \partial\Omega,$$

63 where \mathbf{u} is the unknown solution vector, \mathcal{D} denotes the abstract (non-linear) differ-
 64 ential operator (*e.g.*, $\partial/\partial\mathbf{x}$, $\mathbf{u} \circ \partial/\partial\mathbf{x}$, $\mathbf{x} \circ \partial/\partial\mathbf{x}$, higher order derivatives, non-linear
 65 functions of \mathbf{u} or \mathbf{x} , their combinations, *etc.*), and the operator \mathcal{B} expresses arbitrary
 66 boundary conditions (*e.g.*, Dirichlet, Neumann, Robin, *etc.*) associated with the prob-
 67 lem. Note here for time-dependent problems, we consider t as a special component
 68 of \mathbf{x} , *i.e.*, the Ω contains the temporal domain. The initial condition can be sim-
 69 ply treated as a special type of Dirichlet boundary condition on the spatio-temporal
 70 domain [24].

71 Now we construct a neural network with L layers, or $L - 1$ hidden layers to
 72 approximate $\mathbf{u}(\mathbf{x})$, the input to neural network is \mathbf{x} , and we will denote the output
 73 of the neural network as $\hat{\mathbf{u}}(\mathbf{x}; \theta)$ (we want $\hat{\mathbf{u}}(\mathbf{x}; \theta) \approx \mathbf{u}(\mathbf{x})$), where θ represents
 74 the collection of weight matrix $W^{[l]} \in \mathbf{R}^{n_l \times n_{l-1}}$ and bias vector $b^{[l]} \in \mathbf{R}^{n_l}$ for each
 75 layer l with n_l neurons. In the inverse or data discovery problems, there are some
 76 unknown parameters γ in the original differential equations, thus we will rewrite our
 77 approximation as $\hat{\mathbf{u}}(\mathbf{x}; \theta, \gamma)$. Now we can define the physics-informed loss \mathcal{L} as

$$78 \quad (3.3) \quad \mathcal{L}(\theta, \gamma) = w_f \mathcal{L}_f(\theta, \gamma) + w_b \mathcal{L}_b(\theta, \gamma) + w_d \mathcal{L}_d(\theta, \gamma),$$

79 where w_f is the weight for the loss due to mismatch with the governing equations

$$80 \quad (3.4) \quad \mathcal{L}_f(\theta, \gamma) = \frac{1}{|\Gamma_f|} \sum_{\mathbf{x} \in \Gamma_f \subset \Omega} \|\mathcal{D}(\hat{\mathbf{u}}(\mathbf{x}; \theta, \gamma))\|_2^2,$$

81 and w_b is the weight for the loss due to mismatch with the boundary conditions

$$82 \quad (3.5) \quad \mathcal{L}_b(\theta, \gamma) = \frac{1}{|\Gamma_b|} \sum_{\mathbf{x} \in \Gamma_b \subset \partial\Omega} \|\mathcal{B}(\hat{\mathbf{u}}(\mathbf{x}; \theta, \gamma))\|_2^2,$$

83 and w_d is the weight for the loss due to mismatch with the given data observations
 84 $\mathbf{u}^*(\mathbf{x})$

85 (3.6)
$$\mathcal{L}_d(\theta, \gamma) = \frac{1}{|\Gamma_d|} \sum_{\mathbf{x} \in \Gamma_d \subset \Omega} \|\hat{\mathbf{u}}(\mathbf{x}; \theta, \gamma) - \mathbf{u}^*(\mathbf{x})\|_2^2.$$

86 In practice, Γ_f and Γ_b are always known as the set of locations of the “residual”
 87 points, and Γ_d is known as the set of measurement locations. We then optimize θ and
 88 γ together, and our solution is

89 (3.7)
$$\theta^*, \gamma^* = \underset{\theta, \gamma}{\operatorname{argmin}} \mathcal{L}(\theta, \gamma).$$

90 Above process is approximately summarized in Fig. 1. Due to the network architecture
 91 and incorporation of differential equations, the loss will be highly non-linear and
 92 also non-convex, thus we will need some gradient-based optimizers, such as steepest
 93 descent [4], Newton’s method [4], Adam [20], and L-BFGS (limited-memory quasi-
 94 Newton method) [5]. In this report, we will adopt purely Adam or Adam combined
 95 with L-BFGS optimizers (*i.e.*, we first use Adam for a certain number of iterations,
 and then switch to L-BFGS until convergence).

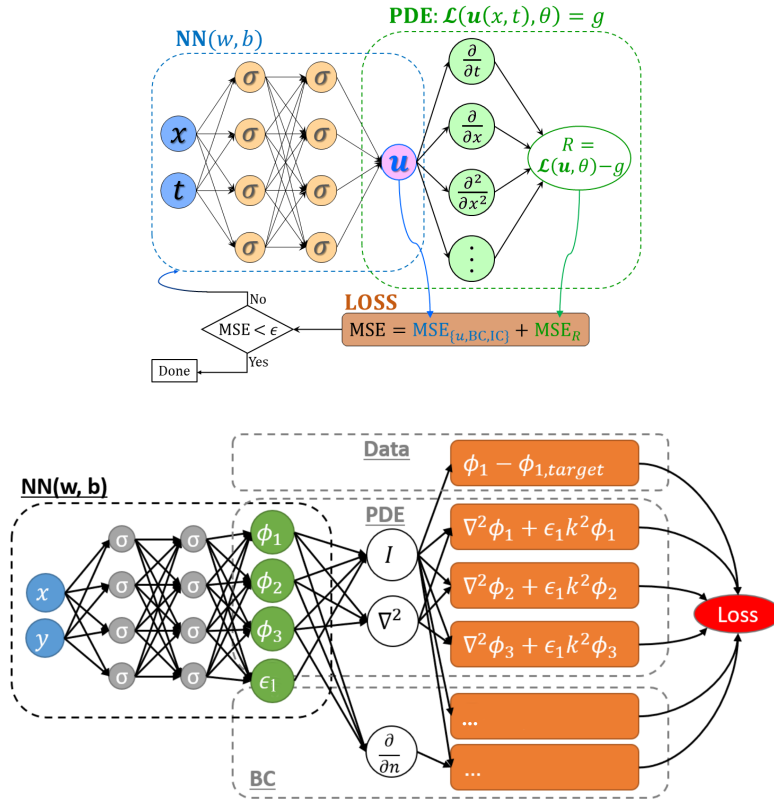


FIG. 1. Two schematics of the physics-informed neural network (PINN) [24, 25].

96 For estimation of the test error, we will evaluate the loss \mathcal{L}_f on a given test set
 97 $\Gamma_{\text{test}} \subset \Omega$. In addition, if the true solution is available, we will also calculate the mean
 98 square error (similar to the form of \mathcal{L}_d) on the same test set.
 99

100 **4. Experiments, results and discussions.**

101 **4.1. One dimensional consolidation problem.** In soil mechanics, one of the
 102 most important processes is the consolidation process, while under some specific as-
 103 sumptions made by Prof. Terzaghi and Prof. Biot [6, 8, 37], we can mathematically
 104 quantify this process as a one dimensional diffusion problem [14] with specific bound-
 105 ary conditions and initial conditions. Suppose our problem domain is $0 \leq x \leq L$
 106 where L can be understood as the thickness of the aquifer that rests on a rigid imper-
 107 meable base, at time $t = 0$, surface load p_0 is applied on the top of the aquifer which
 108 will lead to an initial pore pressure field $p^u = \gamma_l p_0$ at $t = 0^+$ where γ_l is called loading
 109 efficiency [37]. As time goes on, the pressure p will gradually decrease due to the
 110 effect of the drainage boundary at $x = 0$, and it satisfies following partial differential
 111 equation

112 (4.1)
$$\frac{\partial p}{\partial t} - c \frac{\partial^2 p}{\partial x^2} = 0,$$

113 with boundary conditions $p = 0$ at $x = 0$ and $\partial p / \partial x = 0$ at $x = L$. The initial
 114 condition is just $p = p^u$ as mentioned before. In above Eq. (4.1), the c is called
 115 generalized consolidation coefficient [11] which has the unit of length squared divided
 116 by time.

117 However, the order of magnitudes of different physical quantities x (order of
 118 meters), t (order of months) and p (order of kPa) could cast great difficulty on the
 119 training of the neural networks [21], and to overcome this problem, we employ a non-
 120 dimensionalization technique with the purpose of scaling the input and the output
 121 of the neural network in proper scales (*e.g.*, $\mathcal{O}(1)$). As a result, we will introduce
 122 characteristic values for x and p , and for this problem an obvious choice would be
 123 characteristic length L and characteristic pressure p^u . At this point we define the
 124 dimensionless quantities as

125 (4.2)
$$\hat{x} = \frac{x}{L} \quad \hat{p} = \frac{p}{p^u}.$$

126 For the time t , the dimensionless time \hat{t} is given as

127 (4.3)
$$\hat{t} = \frac{ct}{L^2}.$$

128 Now all the variables take values with $\mathcal{O}(1)$ magnitude and we will rewrite Eq. (4.1)
 129 using dimensionless variables, the result is shown as follows

130 (4.4)
$$\begin{aligned} \frac{\partial \hat{p}}{\partial \hat{t}} - \frac{\partial^2 \hat{p}}{\partial \hat{x}^2} &= 0 & 0 < \hat{x} < 1 & \quad \hat{t} > 0 \\ \hat{p} &= 0 & \hat{x} = 0 & \quad \hat{t} \geq 0 \\ \frac{\partial \hat{p}}{\partial \hat{x}} &= 0 & \hat{x} = 1 & \quad \hat{t} > 0 \\ \hat{p} &= 1 & 0 < \hat{x} \leq 1 & \quad \hat{t} = 0. \end{aligned}$$

131 The analytical solution for Eq. (4.4) is given as

132 (4.5)
$$\hat{p} = \sum_{m=1,3,5,7,\dots}^{\infty} \frac{4}{m\pi} \sin\left(\frac{m\pi\hat{x}}{2}\right) e^{-\frac{m^2\pi^2\hat{t}}{4}}.$$

133 For the PINN hyper-parameters, we assume $\hat{t}_{\max} = 0.5$, and we draw 500, 250,
134 125 “residual” points randomly from $(0, 1) \times (0, \hat{t}_{\max})$, boundary of \hat{x} and boundary
135 of \hat{t} respectively to form Γ_f and Γ_b . The test set Γ_{test} will have 10011 points. The
136 loss weights are assigned as $w_f = w_b = 1/4$ (w_d is not used in this problem). For
137 the architecture of the neural network, it will contain 5 hidden layers with 50 neurons
138 each, and we will use hyperbolic tangent `tanh` as our activation function in hidden
139 layers, the output activation will be linear activation but we will multiply the network
140 output with \hat{x} as our final output, because in this way our output will automatically
141 satisfy the second expression in Eq. (4.4). For the optimization procedure, we will
142 run Adam for 50000 epochs with learning rate 0.001 and then run L-BFGS until
143 convergence. For the network initialization, we will use the Glorot normal initializer.
144 The convergence history, reference solution, PINN solution, and the absolute error
145 is shown in the Fig. 2, from which we can see a perfect match is achieved, and the
146 locations with highest error is close to the origin due to sharp gradient. Note in Fig. 2,
147 we have enforced all the output values are between 0 and 1, and initial condition is
strictly satisfied.

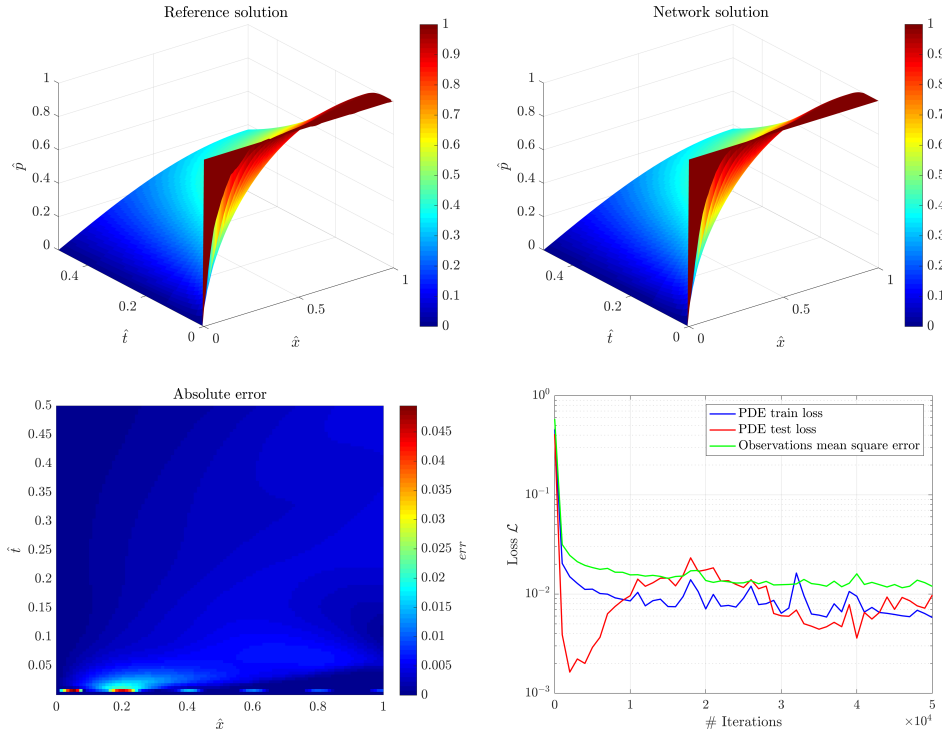


FIG. 2. PINN training results for the one dimensional consolidation problem.

148

149 **4.2. Steady state heat conduction problem.** Our second example is a time-
150 independent problem on 2D. In the steady state heat transfer problem with constant
151 heat conduction coefficient, constant heat source and constant boundary temperature
152 (Dirichlet boundary condition), the T will satisfy Poisson’s equation [14]. Without
153 loss of generality and to avoid the scaling differences, we will solve following PDE on

154 $\Omega = [-1, 1] \times [-1, 1]$

155 (4.6)
$$\frac{\partial^2 T}{\partial x^2} + \frac{\partial^2 T}{\partial y^2} + 1 = 0 \quad -1 < x < 1 \quad -1 < y < 1,$$

156

157 (4.7)
$$T = 0 \quad (x, y) \in \partial\Omega.$$

158 Even though the analytical solution for this problem doesn't exist, the finite element
 159 solution with high accuracy is available in [deal.II finite element library tutorial 3](#), thus
 160 it will be interesting to compare these two numerical solutions.

161 For the PINN hyper-parameters, we choose 1500 and 500 random points to form
 162 Γ_f and Γ_b , respectively. The test set Γ_{test} will have 10000 points. The loss weights are
 163 assigned as $w_f = w_b = 1/2$ (w_d is not used in this problem). For the architecture of
 164 the neural network, it will contain 4 hidden layers with 50 neurons each, and we will
 165 not apply any transform for the network output. The learning rate for this problem
 166 is 0.0005. For the network initialization, we will use the Glorot uniform initializer.
 167 The remaining settings are the same as the first example.

168 The training results are shown in the Fig. 3, where the two numerical solutions
 169 are consistent with each other. Note in Fig. 3, we have enforced all the output values
 170 are larger than 0. The largest absolute error happens near the Dirichlet boundary
 171 because Eq. (4.7) is not regarded as a hard constrain in the construction of the loss
 172 \mathcal{L} . A feasible way to handle this problem would be to introduce a **smooth** distance
 173 function $\hat{d}(\mathbf{x})$ that gives the distance for $\mathbf{x} \in \Omega$ to $\partial\Omega$ [3], and then we multiply \hat{d} with
 174 the original network output to get our new improved output, which will automatically
 175 satisfy Eq. (4.7).

176 **4.3. Inverse problem for simple structural dynamic system.** The last
 177 example comes from the dynamic response of the single degree of freedom system
 178 [10] and we want to use this example to illustrate the capability of PINN in the
 179 inverse modeling or data discovery process. In structural dynamics, the free vibration
 180 equation with viscous damping for single mass point is obtained through D'Alembert
 181 principle [10]

182 (4.8)
$$m \frac{d^2 u}{dt^2} + c \frac{du}{dt} + ku = 0 \quad t > 0$$

183 with $u(0) = u_0$ and $\dot{u}(0) = v_0$. In above equation, $m > 0$ is the mass, $c > 0$ is
 184 the damping coefficient, $k > 0$ is the stiffness, u is the displacement, u_0 is the initial
 185 displacement and v_0 is the initial velocity. The analytical solution to this ODE is
 186 given as

187 (4.9)
$$u(t) = e^{-\xi\omega_n t} \left[u_0 \cos(\omega_D t) + \frac{v_0 + \xi\omega_n u_0}{\omega_D} \sin(\omega_D t) \right],$$

188 where $\omega_n = \sqrt{k/m}$ is known as the natural frequency, $\xi = c/(2m\omega_n)$ is known as
 189 the damping ratio, $\omega_D = \omega_n \sqrt{1 - \xi^2}$. In this problem, we will assume $\xi < 1$ which is
 190 known as the underdamped system.

191 Now suppose $m = u_0 = v_0 = 1$, c and k are the two parameters to be identified
 192 from the observations at certain times. The observations are produced with the un-
 193 derlying true parameters $c = 0.4$ and $k = 4$ using Eq. (4.9). We choose 50 equispaced
 194 points to form Γ_d , 100 random points to form Γ_f , 50 random points to form Γ_b and

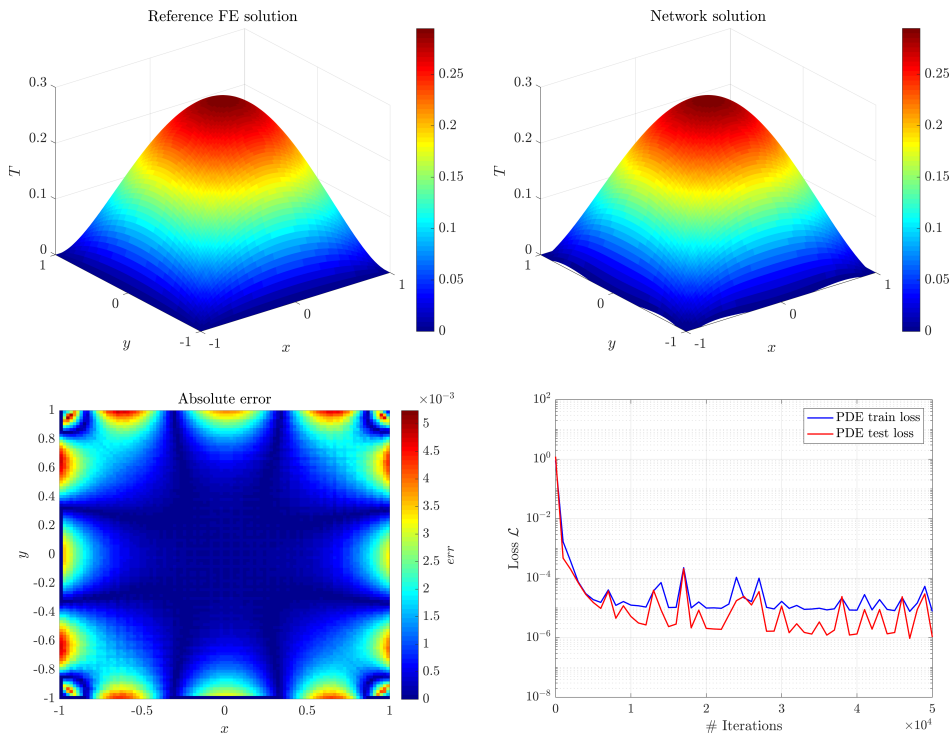


FIG. 3. PINN training results for the steady state heat conduction problem.

195 10000 points to form Γ_{test} . The loss weights are assigned as $w_f = w_b = w_d = 1/4$.
 196 For the architecture of the neural network, it will contain 3 hidden layers with 32
 197 neurons each, and we will not apply any transform for the network output. For the
 198 optimization procedure, we will only run Adam for 100000 epochs with learning rate
 199 0.0005. For the network initialization, we will use the Glorot uniform initializer.

200 The evolution trajectories of c and k are presented in Fig. 4, with final values of
 201 $\bar{k} = 3.9933197$ and $\bar{c} = 0.40125215$, which agree with their true values.

202 **5. Conclusions.** In this project, we have adopted PINN, a new class of univer-
 203 sal function approximators that is capable of encoding any underlying conservation
 204 laws which can be described by differential equations. Compared to the traditional
 205 numerical methods, PINN employs automatic differentiation to handle differential op-
 206 erators, and thus are mesh-free. We use PINN as a data driven algorithm for inferring
 207 solutions and parameter identifications of differential equations. A series of promising
 208 results for a diverse collection of problems in mechanics are presented and discussed,
 209 which opens the path for endowing deep learning with the powerful capacity of math-
 210 ematical physics to model the world around us. We hope this project could benefit
 211 future practitioners across a wide range of scientific domains who want to incorporate
 212 deep learning methods in modeling physics-related problems.

213 For the future work, it is worth to try a group of coupled differential equations
 214 such as Eqs. (5.1)(5.2) in poromechanics [40] to see the PINN's performance, and
 215 develop some training points selection strategy similar to the adaptive re-meshing in

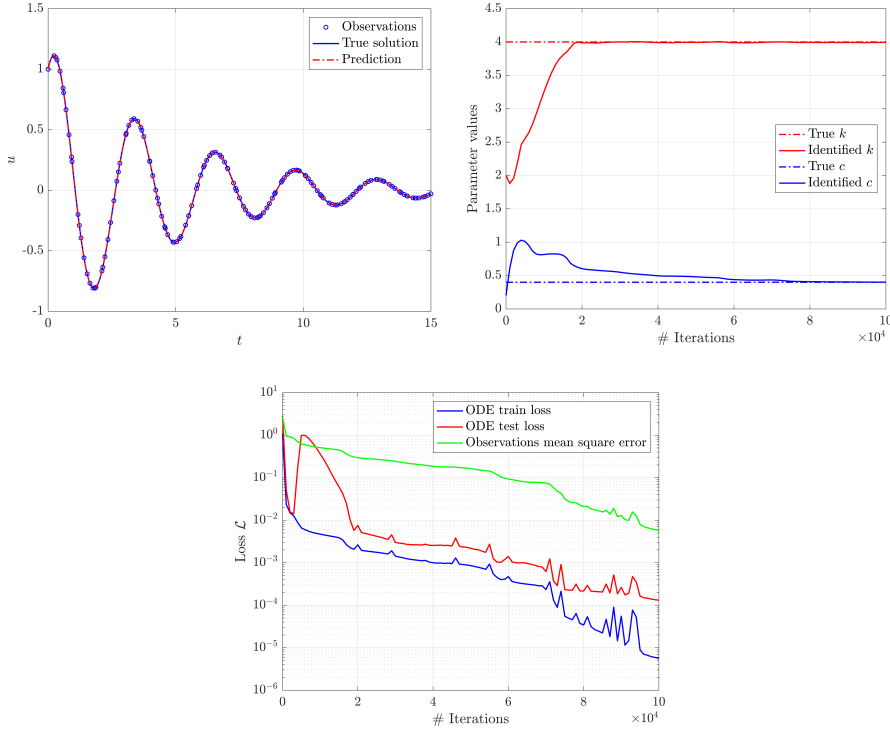


FIG. 4. PINN training results for the parameter identification problem, the identified values converge to the true values during the training process.

216 the mesh-based methods to achieve better accuracy.

$$217 \quad (5.1) \quad \frac{1}{M} \frac{\partial p}{\partial t} - \frac{k}{\mu_f} \nabla^2 p + \alpha \frac{\partial \nabla \cdot \mathbf{u}}{\partial t} = 0,$$

218

$$219 \quad (5.2) \quad G \nabla^2 \mathbf{u} + \frac{G}{1 - 2\nu} \nabla (\nabla \cdot \mathbf{u}) - \alpha \nabla p + \rho_b \mathbf{g} = \mathbf{0}.$$

- 221 [1] Y. BAR-SINAI, S. HOYER, J. HICKEY, AND M. P. BRENNER, *Learning data-driven discretizations*
 222 *for partial differential equations*, Proceedings of the National Academy of Sciences, 116
 223 (2019).
- 224 [2] A. G. BAYDIN, B. A. PEARLMUTTER, A. A. RADUL, AND J. M. SISKIND, *Automatic differ-*
 225 *entiation in machine learning: a survey*, The Journal of Machine Learning Research, 18
 226 (2017).
- 227 [3] J. BERG AND K. NYSTRÖM, *A unified deep artificial neural network approach to partial differ-*
 228 *ential equations in complex geometries*, Neurocomputing, 317 (2018).
- 229 [4] S. BOYD AND L. VANDENBERGHE, *Convex optimization*, Cambridge university press, 2004.
- 230 [5] R. H. BYRD, P. LU, J. NOCEDAL, AND C. ZHU, *A limited memory algorithm for bound con-*
 231 *strained optimization*, SIAM Journal on scientific computing, 16 (1995), pp. 1190–1208.
- 232 [6] N. CASTELLETTO, J. A. WHITE, AND H. A. TCHELEPI, *Accuracy and convergence properties of*
 233 *the fixed-stress iterative solution of two-way coupled poromechanics*, International Journal
 234 for Numerical and Analytical Methods in Geomechanics, 39 (2015).
- 235 [7] X. CHEN, J. DUAN, AND G. E. KARNIADAKIS, *Learning and meta-learning of sto-*
 236 *chastic advection-diffusion-reaction systems from sparse measurements*, arXiv preprint
 237 arXiv:1910.09098, (2019).
- 238 [8] A. H. D. CHENG, *Poroelasticity*, Springer, 2016.
- 239 [9] M. CHIARAMONTE AND M. KIENER, *Solving differential equations using neural networks*, CS229
 240 Project, (2013).
- 241 [10] A. K. CHOPRA, *Dynamics of structures: theory and applications to earthquake engineering*,
 242 Prentice Hall, 1995.
- 243 [11] E. DETOURNAY AND A. H. D. CHENG, *Fundamentals of poroelasticity*, in Analysis and design
 244 methods, Elsevier, 1993, pp. 113–171.
- 245 [12] M. W. M. G. DISSANAYAKE AND N. PHAN-THIEN, *Neural-network-based approximations for*
 246 *solving partial differential equations*, Communications in Numerical Methods in Engineer-
 247 ing, 10 (1994), pp. 195–201.
- 248 [13] T. DOCKHORN, *A discussion on solving partial differential equations using neural networks*,
 249 arXiv preprint arXiv:1904.07200, (2019).
- 250 [14] L. C. EVANS, *Partial differential equations*, American Mathematical Society, 2010.
- 251 [15] J. GHABOUSSI, J. H. GARRETT JR, AND X. WU, *Knowledge-based modeling of material behavior*
 252 *with neural networks*, Journal of engineering mechanics, 117 (1991).
- 253 [16] E. HAGHIGHAT, M. RAISSI, A. MOURE, H. GOMEZ, AND R. JUANES, *A deep learning frame-*
 254 *work for solution and discovery in solid mechanics: linear elasticity*, arXiv preprint
 255 arXiv:2003.02751, (2020).
- 256 [17] J. HAN, A. JENTZEN, AND E. WEINAN, *Solving high-dimensional partial differential equations*
 257 *using deep learning*, Proceedings of the National Academy of Sciences, 115 (2018).
- 258 [18] Q. HE, D. BARAJAS-SOLANO, G. TARTAKOVSKY, AND A. M. TARTAKOVSKY, *Physics-informed*
 259 *neural networks for multi-physics data assimilation with application to subsurface trans-*
 260 *port*, Advances in Water Resources, (2020), p. 103610.
- 261 [19] T. KADEETHUM, T. M. JØRGENSEN, AND H. M. NICK, *Physics-informed neural networks for*
 262 *solving nonlinear diffusivity and biot’s equations*, PloS one, 15 (2020), p. e0232683.
- 263 [20] D. P. KINGMA AND J. BA, *Adam: A method for stochastic optimization*, arXiv preprint
 264 arXiv:1412.6980, (2014).
- 265 [21] G. KISSAS, Y. YANG, E. HwuANG, W. R. WITSCHey, J. A. DETRE, AND P. PERDIKARIS,
 266 *Machine learning in cardiovascular flows modeling: Predicting arterial blood pressure from*
 267 *non-invasive 4d flow mri data using physics-informed neural networks*, Computer Methods
 268 in Applied Mechanics and Engineering, 358 (2020).
- 269 [22] I. E. LAGARIS, A. LIKAS, AND D. I. FOTIADIS, *Artificial neural networks for solving ordinary*
 270 *and partial differential equations*, IEEE transactions on neural networks, 9 (1998).
- 271 [23] M. LEFIK, D. P. BOSO, AND B. A. SCHREFLER, *Artificial neural networks in numerical model-*
 272 *ling of composites*, Computer Methods in Applied Mechanics and Engineering, 198 (2009).
- 273 [24] L. LU, X. MENG, Z. MAO, AND G. E. KARNIADAKIS, *DeepXDE: A deep learning library for*
 274 *solving differential equations*, arXiv preprint arXiv:1907.04502, (2019).
- 275 [25] X. MENG, Z. LI, D. ZHANG, AND G. E. KARNIADAKIS, *Ppinn: Parareal physics-informed neural*
 276 *network for time-dependent pdes*, arXiv preprint arXiv:1909.10145, (2019).
- 277 [26] M. MOZAFFAR, R. BOSTANABAD, W. CHEN, K. EHMANN, J. CAO, AND M. A. BESSA, *Deep learn-*
 278 *ing predicts path-dependent plasticity*, Proceedings of the National Academy of Sciences,
 279 116 (2019).
- 280 [27] M. RAISSI, *Deep hidden physics models: Deep learning of nonlinear partial differential equa-*

- 281 *tions*, The Journal of Machine Learning Research, 19 (2018), pp. 1–24.
- 282 [28] M. RAISSI AND G. E. KARNIADAKIS, *Hidden physics models: Machine learning of nonlinear*
283 *partial differential equations*, Journal of Computational Physics, 357 (2018), pp. 125–141.
- 284 [29] M. RAISSI, P. PERDIKARIS, AND G. E. KARNIADAKIS, *Machine learning of linear differential*
285 *equations using gaussian processes*, Journal of Computational Physics, 348 (2017), pp. 683–
286 693.
- 287 [30] M. RAISSI, P. PERDIKARIS, AND G. E. KARNIADAKIS, *Physics informed deep learning (part*
288 *i): data-driven solutions of nonlinear partial differential equations*, arXiv preprint
289 arXiv:1711.10561, (2017).
- 290 [31] M. RAISSI, P. PERDIKARIS, AND G. E. KARNIADAKIS, *Physics informed deep learning (part*
291 *ii): data-driven discovery of nonlinear partial differential equations*, arXiv preprint
292 arXiv:1711.10566, (2017).
- 293 [32] M. RAISSI, P. PERDIKARIS, AND G. E. KARNIADAKIS, *Physics-informed neural networks: A deep*
294 *learning framework for solving forward and inverse problems involving nonlinear partial*
295 *differential equations*, Journal of Computational Physics, 378 (2019), pp. 686–707.
- 296 [33] J. SIRIGNANO AND K. SPILIOPOULOS, *Dgm: A deep learning algorithm for solving partial dif-*
297 *ferential equations*, Journal of Computational Physics, 375 (2018), pp. 1339–1364.
- 298 [34] Y. SUN, W. ZENG, Y. ZHAO, X. ZHANG, Y. SHU, AND Y. ZHOU, *Modeling constitutive relation-*
299 *ship of ti40 alloy using artificial neural network*, Materials & Design, 32 (2011).
- 300 [35] A. TARTAKOVSKY, C. O. MARRERO, P. PERDIKARIS, G. TARTAKOVSKY, AND D. BARAJAS-
301 SOLANO, *Physics-informed deep neural networks for learning parameters and constitutive*
302 *relationships in subsurface flow problems*, Water Resources Research, 56 (2020).
- 303 [36] J. TOMPSON, K. SCHLACHTER, P. SPRECHMANN, AND K. PERLIN, *Accelerating eulerian fluid*
304 *simulation with convolutional networks*, in Proceedings of the 34th International Confer-
305 ence on Machine Learning, 2017.
- 306 [37] H. F. WANG, *Theory of linear poroelasticity with applications to geomechanics and hydrogeol-*
307 *ogy*, Princeton University Press, 2000.
- 308 [38] E. WEINAN, J. HAN, AND A. JENTZEN, *Deep learning-based numerical methods for high-*
309 *dimensional parabolic partial differential equations and backward stochastic differential*
310 *equations*, Communications in Mathematics and Statistics, 5 (2017), pp. 349–380.
- 311 [39] E. WEINAN AND B. YU, *The deep ritz method: a deep learning-based numerical algorithm for*
312 *solving variational problems*, Communications in Mathematics and Statistics, 6 (2018),
313 pp. 1–12.
- 314 [40] Q. ZHANG, J. CHOO, AND R. I. BORJA, *On the preferential flow patterns induced by transverse*
315 *isotropy and non-darcy flow in double porosity media*, Computer Methods in Applied Me-
316 chanics and Engineering, 353 (2019), pp. 570–592.